Quantum Data Compression of a Qubit Ensemble

Lee A. Rozema,[1,*] Dylan H. Mahler,[1] Alex Hayat,[1,2,3] Peter S. Turner,[4,†] and Aephraim M. Steinberg[1,3]
[1]Centre for Quantum Information and Quantum Control and Department of Physics, University of Toronto, 60 Saint George Street, Toronto, Ontario M5S 1A7, Canada
[2]Department of Electrical Engineering, Technion, Haifa 32000, Israel
[3]Canadian Institute for Advanced Research, Toronto, Ontario M5G 1Z8, Canada
[4]Department of Physics, Graduate School of Science, University of Tokyo, 7-3-1 Hongo, Bunkyo-ku, Tokyo 113-0033, Japan
(Received 3 July 2014; published 17 October 2014)

Data compression is a ubiquitous aspect of modern information technology, and the advent of quantum information raises the question of what types of compression are feasible for quantum data, where it is especially relevant given the extreme difficulty involved in creating reliable quantum memories. We present a protocol in which an ensemble of quantum bits (qubits) can in principle be perfectly compressed into exponentially fewer qubits. We then experimentally implement our algorithm, compressing three photonic qubits into two. This protocol sheds light on the subtle differences between quantum and classical information. Furthermore, since data compression stores all of the available information about the quantum state in fewer physical qubits, it could allow for a vast reduction in the amount of quantum memory required to store a quantum ensemble, making even today's limited quantum memories far more powerful than previously recognized.

DOI: 10.1103/PhysRevLett.113.160504 PACS numbers: 03.67.Ac, 42.50.Ex

The amount of information that can be extracted from a classical system is precisely the same as the amount of information required for a complete description of the system's state. The same is not true quantum mechanically; to fully describe the state of a single quantum bit (qubit) would require an infinite amount of information, although no more than one (classical) bit of information can ever be extracted from a measurement of its quantum state. Such fundamental differences between quantum and classical mechanics open up the possibility of new kinds of data compression with no classical analogue. In quantum mechanics an ensemble of identically prepared quantum systems provides much more information than a single copy—this is not the case classically, where the information encoded in a single system's state can be accessed repeatedly. Although quantum mechanically we cannot compress all of the information contained in an ensemble of systems down to a single quantum copy, we can achieve an exponential savings. In this Letter, we show how this exponential savings can be realized using the quantum Schur-Weyl transform [1,2], which can compress an ensemble of N identically prepared qubits into a memory of size $\log_2[N+1]$ qubits. We show how the protocol can be made practical in an optical setting, experimentally implementing a three-qubit quantum circuit to compress a three-qubit ensemble into the state of two qubits. To characterize this circuit, we show that we can perform measurements on the two compressed qubits, and still extract as much information as we would have been able to given all three original qubits. Given our ability to extract information about measurements in multiple bases, we can conclude that the compressed state faithfully encodes the "quantum information content" of the original ensemble. Our results demonstrate that quantum memories can store exponentially more information about a quantum state than would normally be expected for the number of physical qubits that the memory can hold.

From the point of view of estimation theory, a quantum state is never fully knowable, just as a classical probability distribution is not fully knowable (both would require infinite resources). Hence, for our purposes, a quantum state is best thought of as an object that allows one to make testable predictions about the statistics of potential measurements done on a large ensemble of identically prepared systems. Thus "quantum state estimation" is really the task of making predictions about the expectation values for observables that might be measured in the future. Consider for instance estimating the spin projection of a qubit along a particular direction, given a fixed number of identically prepared qubits. The best strategy is simply to measure the spin along the direction of interest on each copy and draw conclusions as one would do classically. Clearly, having more copies allows for a better estimate. If the measurement of interest is unknown, however, the standard approach is to reconstruct a density matrix [3], containing enough information to estimate any expectation value. This has the disadvantage that no single estimate can ever make optimal use of all of the information [4]. For instance, in single-qubit tomography one most commonly splits an initial ensemble of identical qubits into three groups, and measures $\hat{X}$ on all the members of one group, $\hat{Y}$ on another, and $\hat{Z}$ on the last. But if, for example, one later wishes to

estimate $\langle\hat{Z}\rangle$ (the expectation value of the spin along $\hat{Z}$), the measurements of $\hat{X}$ and $\hat{Y}$ give no useful information, and two thirds of the measurements have been wasted. In fact, on average, the estimate will be only as accurate as if about one third of the ensemble had been measured; this is the price one pays for the generality of tomography: one has information about all three axes, but only one third as much information about each (the situation becomes more dire in higher dimensions). A better estimate of the spin along any specific direction could be made if one held on to the initial ensemble—requiring a quantum memory—until one knew the measurement of interest. Thus, storing all of the qubits would enable the most accurate predictions about any single measurement. In the classical case, an identically prepared ensemble of bits is highly redundant, so that ideally the information can be compressed down to one bit. This redundancy, along with the challenge of building quantum memories, motivates the question: how many qubits must we store to achieve the same prediction accuracy that is possible with the initial ensemble?

The dimension of the Hilbert space of an N-qubit system grows exponentially in the number of qubits, that is, as 2^N. However, the state of an ensemble of N identically prepared (pure) qubits is the tensor product of N identical pure states, and lives in the $(N+1)$-dimensional fully symmetric subspace. Such N-qubit states can be described using $N+1$ rather than 2^N dimensions because the vast majority of the information in a general multiqubit state describes permutations, which are irrelevant for an ensemble of identical qubits. The remainder of the information describes the effective angular momentum of the multiqubit state, and is the only information relevant to estimating expectation values of single-qubit observables. Thus it is natural to ask if the initial N-qubit ensemble can be mapped reversibly (unitarily) onto exponentially fewer ($\log_2[N+1]$) qubits. In fact, this mapping of the computational basis into a new basis, separating the permutation from the angular momentum information, is well understood as the quantum Schur-Weyl transform (QSWT) [1], and has been theoretically proposed for use in a variety of different applications [2,5–9]. In this Letter we develop a practical scheme for implementing the QSWT, and experimentally demonstrate it with photonic qubits, compressing a three-qubit ensemble into two qubits. (The compression of a quantum ensemble is very different from, and should not be confused with, quantum source coding [10,11].)

A three-qubit QSWT will compress an ensemble of three qubits into two ($\log_2[3+1]$) qubits, so that one qubit can be discarded without information loss. A quantum circuit implementing the three-qubit QSWT is shown in Fig. 1(a). In this circuit, the two single-qubit unitaries, $\hat{U}_1$ and $\hat{U}_2$, are defined so that $\hat{U}_1(\sqrt{(2/3)}|0\rangle+\sqrt{(1/3)}|1\rangle)=|0\rangle$, $\hat{U}_2(\sqrt{(1/3)}|0\rangle+\sqrt{(2/3)}|1\rangle)=|0\rangle$ and $\hat{U}_2\hat{U}_1=\hat{X}$. It is straightforward to show that if the three input qubits

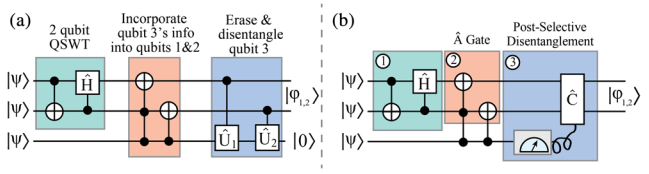

FIG. 1 (color online). (a) Quantum Schur-Weyl transform. A three-qubit quantum Schur-Weyl transform. $\hat{U}_1$ and $\hat{U}_2$ are unitaries (whose detailed descriptions can be found in the main text) which are controlled by the upper qubit; the H is a controlled Hadamard and the other two-qubit gates are CNOTs, while the three-qubit gate is a Toffoli. (b) Simplified circuit. The shaded area labeled 2 can be viewed as a two-qubit unitary gate, $\hat{A}$, acting on the first two qubits which is controlled by the third qubit. C is a two-qubit unitary gate which is applied (or not) based on a measurement of qubit 3. The numbered boxes correspond to the areas in Fig. 2 which show the physical implementation of the circuit elements.

are prepared in $|\psi\rangle=\alpha|0\rangle+\beta|1\rangle$ the output will be transformed into $|\phi\rangle_{1,2}|0\rangle_3$, where

$$|\phi\rangle_{1,2}=\alpha^3|00\rangle+\sqrt{3}\alpha^2\beta|01\rangle+\sqrt{3}\alpha\beta^2|10\rangle+\beta^3|11\rangle. \quad (1)$$

Since the third qubit is always in $|0\rangle$ this circuit unitarily maps all of the information onto the first two qubits. (Such circuits can be efficiently made for any value of N, requiring one to keep only $\log_2[N+1]$ qubits [1,2].) In the case of identical pure-state qubits the final two disentangling gates can be implemented using measurement and feedforward, as shown in Fig. 1(b) [12]. Now qubit 3 is measured and an operation is performed on the first two qubits which depends on this result. This simplification produces $|\phi\rangle_{1,2}$, and thus performs as well as the full QSWT [13].

To understand why the compression of an ensemble of three identical qubits into two does not lose information, consider how one would estimate $\langle\hat{Z}\rangle$ (which we will refer to as Z_{true}, the "true value" of this expectation value) with and without quantum data compression. In short, without compression each qubit is measured in the same basis and an estimate is calculated from a tally of the number of spin-up and spin-down measurement results. This tally is an integer between 0 and N, and can therefore be written as a ($\log_2[N+1]$)-bit string. Explicitly, $\hat{Z}$ is measured on the three qubits, and Z_{true} is estimated directly from the individual outcomes $Z_i=\pm1/2$ as $Z_{\text{direct}}=(Z_1+Z_2+Z_3)/3$. Z_{direct} has four possible values, given by the number of spin-up measurement results, which can be 3, 2, 1, or 0, corresponding to maximum-likelihood estimates of $Z_{\text{direct}}=\{+1/2,+1/6,-1/6,-1/2\}$, respectively. Since the permutation information (which qubits came out spin-up or spin-down) is irrelevant there are $N+1$ (four) rather than 2^N (eight) outcomes. The QSWT removes this irrelevant permutation information, compressing an

$(N+1)$-valued outcome from a (2^N)-into an $(N+1)$-dimensional system. Quantum data compression amounts to encoding this information directly in $(\log_2[N+1])$ qubits, discarding the rest; so as long as the coherence between all such states is preserved, the resulting quantum state faithfully preserves the statistics of such tallies in all bases. With quantum data compression, Z_{true} is estimated by measuring both compressed qubits and computing $Z_{\text{comp}} = (2Z_1 + Z_2)/3$ (which can take the same four values as Z_{direct}). To quantify the quality of the two estimates, Z_{direct} and Z_{comp}, we compare their statistical variances (since the expectation values of both estimates are equal to Z_{true}, their variances are equivalent to their mean-squared error). For the single-qubit state $\alpha|0\rangle + \beta|1\rangle$, both Z_{direct} and Z_{comp} have variances of $|\alpha|^2|\beta|^2/3$ (as expected, given that spin measurements obey binomial statistics). These identical statistics indicate that there is just as much information about Z_{true} in the two compressed qubits as there is in the three uncompressed qubits. More importantly, measurements on the compressed state $|\phi\rangle_{1,2}$ can be used to estimate *any* single-qubit operator with the same statistical uncertainty as a direct measurement [13]. It is in this sense that the two-qubit state $|\phi\rangle_{1,2}$ carries as much information about $|\psi\rangle$ as the three-qubit input $|\psi\rangle^{\otimes 3}$.

To demonstrate this protocol experimentally, we use three qubits, encoded in the path and polarization degrees of freedom of two photons [14,15]. Such hybrid quantum systems, using multiple degrees of freedom of photons, have proven very useful for demonstrating quantum protocols [16–18], testing fundamental issues in quantum mechanics, [19,20], and simplifying quantum logic gates [21,22]. In the circuit of Fig. 1(b), qubit 1 is encoded in the polarization of photon 1, qubit 2 is encoded in an additional path degree of freedom of the same photon, and qubit 3 is encoded in the polarization of a second photon. After the circuit is completed, the information of all three qubits is stored in the first two logical qubits, both encoded in photon 1, allowing us to discard the second photon entirely. A sketch of our optical implementation is shown in Fig. 2, and explained in the Supplemental Material [13]. The two compressed qubits are encoded in the path and polarization of photon 1; to perform the postselective disentanglement, measurements of these two qubits are postselected on a measurement of photon 2. This corresponds to a coincidence event between a measurement on photon 2 signaling $|H + iV\rangle/\sqrt{2}$ and any of the four detectors for photon 1. There are four detectors because there are two possible path outcomes and two possible polarization outcomes. These coincidence events correspond to four different estimates of Z_{true}: $HP_0 = |00\rangle \Rightarrow Z_{\text{comp}} = +1/2$, $HP_1 = |01\rangle \Rightarrow Z_{\text{comp}} = +1/6$, $VP_0 = |10\rangle \Rightarrow Z_{\text{comp}} = -1/6$, or $VP_1 = |11\rangle \Rightarrow Z_{\text{comp}} = -1/2$.

To test the performance of our circuit, the compressed system was measured and a number of representative single-qubit observables were estimated. For each measurement,

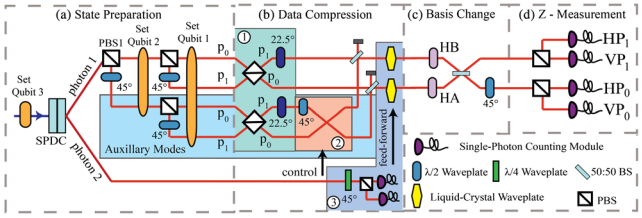

FIG. 2 (color online). Optical Implementation. (a)–(b) State preparation and data compression. Two photons, generated via spontaneous parametric down-conversion (SPDC), are used to encode three qubits. Qubit 1 is encoded in the polarization of photon 1, qubit 2 in its path degree-of-freedom (the logical paths are labeled P_0 and P_1), and qubit 3 in the polarization of photon 2 (initially entangled with an additional path degree of freedom of photon 1). After data compression, only photon 1 remains, encoding a path and polarization qubit. (c)–(d) Measuring the compressed qubits. Any single-qubit measurement can be made on the compressed state in two steps by first setting the basis (c), and then measuring $\hat{Z}$ (d). The $\hat{Z}$ measurement has four outcomes: HP_1, VP_1, HP_0, and VP_1 [where H (V) stands for horizontal (vertical) polarization]. The areas numbered 1–3 correspond to circuit elements shown in Fig. 1(b).

the two qubits were found in one of four states, corresponding to expectation-value estimates of $+1/2, +1/6, -1/6$, or $-1/2$. Since a single measurement does not yield information about the statistical performance of our circuit, we ran the circuit many times for the same input state and final measurement. The number of runs was typically $M \approx 500$. For each run, $\hat{S}$ (either $\hat{X}$, $\hat{Y}$, or $\hat{Z}$) was measured on the output and the spin expectation value was estimated as $S_{\text{comp}} = (2S_1 + S_2)/3$, then the average of S_{comp} over runs was calculated. This entire process formed a single trial, and was repeated about 250 times. The resulting distributions of the averages of S_{comp} are plotted in Figs. 3(a)–3(c) for $\hat{S} = \hat{X}$, $\hat{Y}$, and $\hat{Z}$ with the initial single-qubit state $\cos(2\theta)|0\rangle + \sin(2\theta)|1\rangle$ and $\theta = 13.5°$. If each of the M measurements encodes the information of three qubits (as we expect) the distribution should have a variance given by the single-qubit variance $[V_1 = \cos^2(2\theta)\sin^2(2\theta)]$ divided by the total number of qubits sampled: $3M$, three times the number of runs in each trial. This prediction is shown in blue on Figs. 3(a)–3(c). On the other hand, a measurement made on two independent qubits would exhibit a variance of $V_1/(2M)$, 1.5 times larger; this distribution is shown in red for comparison. The narrower blue curve, describing the behavior of three qubits, is a much better fit to our observed data than the red curve, indicating that the amount of information extractable from the two compressed qubits is close to the full information present in the three original qubits.

To further quantify the performance of our compression circuit, we measure the "single-shot" distributions of X_{comp}, Y_{comp}, and Z_{comp}. To do this we again prepare each of the three input qubits in $\cos(2\theta)|0\rangle + \sin(2\theta)|1\rangle$, run our

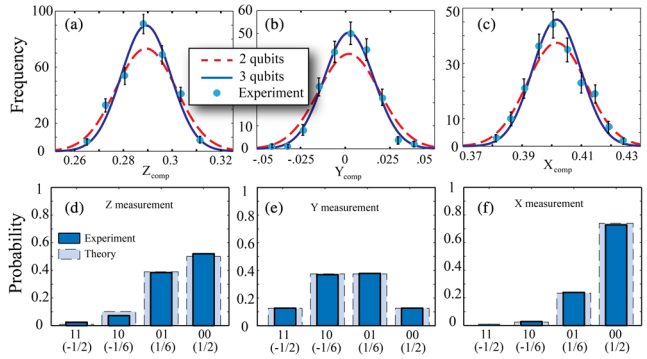

FIG. 3 (color online). Sample raw data for an input state $\cos(2\theta)|0\rangle + \sin(2\theta)|1\rangle$, for $\theta = 13.5°$. (a)–(c) Histograms of estimates the spin along $\hat{Z}$, $\hat{Y}$, and $\hat{X}$, after M trials (defined in the text) of the data compression circuit. The bars are experimentally measured data, and the blue (red) curve is a normal distribution of width $V_1/3M$ ($V_1/2M$) normalized to have the same area as the experimental histogram, where V_1 is the single-qubit variance. (d)–(f) The experimentally observed probabilities for measuring the two qubits and finding them in $|00\rangle$, $|01\rangle$, $|10\rangle$, or $|11\rangle$ for $\hat{Z}$, $\hat{Y}$, and $\hat{X}$ measurements. The dark blue bars are the experimentally measured counts, normalized by the total number of counts, and the light bars are the theoretically predicted results.

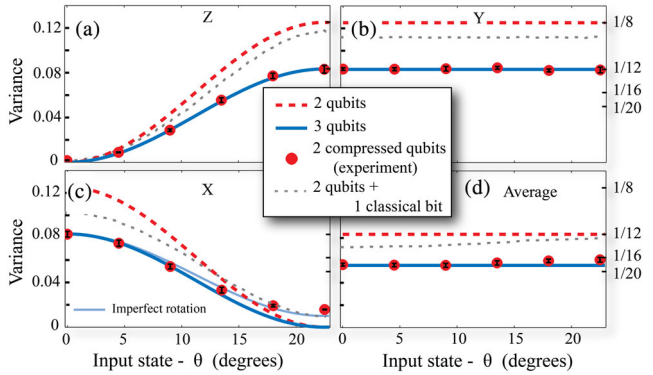

FIG. 4 (color online). Measurement variances for various input states. The solid blue lines are the theoretical variances resulting from performing a measurement on three independent qubits (and thus our two compressed qubits), the dashed red lines are for two independent qubits, the grey dashed lines are the theoretical variance when two independent qubits are measured optimally and a random measurement is performed on a third qubit, and the circles are the variances which we observe when experimentally measuring the two compressed qubits. (a)–(c) By sending in various input states, parameterized as $\cos 2\theta|0\rangle + \sin 2\theta|1\rangle$, we see that the two compressed qubits demonstrate the statistics of three independent qubits for $\hat{Z}$, $\hat{Y}$, and $\hat{X}$ measurements. (d) Averaging the above variances yields the variance averaged over all possible measurements.

circuit, measure one of the observables $\hat{X}$, $\hat{Y}$, or $\hat{Z}$ (each measurement results in an estimate of $+1/2, +1/6, -1/6$, or $-1/2$) and bin the results. For each observable the circuit was run approximately 10^5 times. The resulting normalized distributions are plotted in Figs. 3(d)–3(f) for $\theta = 13.5°$. We observe very good agreement between our experimental data (dark bars) and theory (larger light bars). Next, we vary the input states, preparing a range of θ values, and measure the variance of the resulting single-shot distributions of X_{comp}, Y_{comp}, and Z_{comp} for each input state. These experimentally measured variances are the circles, plotted versus θ, in Figs. 4(a)–4(c). The curves in Figs. 4(a)–4(c) are theory corresponding to the variance of two independent qubits $V_1/2$ (red dashed curve) and three independent qubits $V_1/3$ (blue solid curve). For all but two data points in the $\hat{X}$ measurement (discussed in [13]), our experimental data agree very well with the three-qubit variance. In addition to these three observables, one would ideally quantify the variance averaged over all possible measurements. Such a measurement would indicate how much information could be extracted about arbitrary measurements. Conveniently, for a given state, this average measurement variance is the same as simply averaging the variances of $\hat{X}$, $\hat{Y}$, and $\hat{Z}$. [That is to say that the uniformly distributed discrete subensemble $\{\hat{X}, \hat{Y}, \hat{Z}\}$ is an *averaging set* for the SO(3) uniformly (Haar) distributed superensemble $\{\hat{S}(\theta, \phi)\}$ for variance [13,23]]. The resulting averaged variance is plotted in Fig. 4(d). This clearly demonstrates that our circuit compresses three qubits into two, and we can conclude that all of the compressed states we tested encode the information about *any* single-qubit measurement.

So far we have imagined that, given three qubits and a two-qubit quantum memory, our strategy in the absence of compression would be to store two of the qubits and discard the third. This measurement scheme has a variance 1.5 times larger than we obtain with compression (red curve in Fig. 4). A better approach would be to measure the third qubit before discarding it. The classical bit obtained would provide extra information and could be combined with the subsequent measurement of the two stored qubits in the correct basis, yielding an improved estimate of the single-qubit spin. Any compression algorithm should be compared to such a strategy. We analyze this protocol in [13]; the result is the dotted grey curve in Fig. 4. Our compression scheme outperforms even this improved protocol.

Finally, it is worth mentioning that our techniques could be useful beyond compressing sets of identical input states. For instance, one could also exponentially compress any permutationally invariant pure state. Permutationally invariant states include several entangled states which have been shown to be invaluable for quantum communication and quantum computing [24–26], including GHZ states [27,28] and W states [29]. Many other applications of the QSWT, outside of compression, exist [2,5–9], and for some applications our feedforward simplification performs optimally. Given the exponential reduction in the size of the required quantum memory, and the many applications of the QSWT, circuits such as the one we have demonstrated hold great promise for future quantum computing and communication architectures.

We thank Robin Blume-Kohout for helpful discussions and Alan Stummer for help building our coincidence circuit. L. A. R., D. H. M., A. H., and A. M. S. acknowledge support from the Natural Sciences and Engineering Research Council of Canada and the Canadian Institute for Advanced Research, and P. S. T. acknowledges the support of a *wakatehake* travel grant from the University of Tokyo.

*Corresponding author.
lrozema@physics.utoronto.ca
†Present address: H. H. Wills Laboratory, School of Physics, University of Bristol, Bristol BS8 1TL, United Kingdom.

[1] D. Bacon, I. L. Chuang, and A. W. Harrow, Phys. Rev. Lett. **97**, 170502 (2006).
[2] M. Plesch and V. Bužek, Phys. Rev. A **81**, 032317 (2010).
[3] D. F. V. James, P. G. Kwiat, W. J. Munro, and A. G. White, Phys. Rev. A **64**, 052312 (2001).
[4] R. Blume-Kohout, New J. Phys. **12**, 043034 (2010).
[5] I. Marvian and R. W. Spekkens, arXiv:1112.0638.
[6] M. Keyl and R. F. Werner, Phys. Rev. A **64**, 052311 (2001).
[7] M. Hayashi and K. Matsumoto, Phys. Rev. A **66**, 022311 (2002).
[8] J. Eisert, T. Felbinger, P. Papadopoulos, M. B. Plenio, and M. Wilkens, Phys. Rev. Lett. **84**, 1611 (2000).
[9] S. D. Bartlett, T. Rudolph, and R. W. Spekkens, Phys. Rev. Lett. **91**, 027901 (2003).
[10] B. Schumacher, Phys. Rev. A **51**, 2738 (1995).
[11] Y. Mitsumori, J. Vaccaro, S. Barnett, E. Andersson, A. Hasegawa, M. Takeoka, and M. Sasaki, Phys. Rev. Lett. **91**, 217902 (2003).
[12] R. B. Griffiths and C.-S. Niu, Phys. Rev. Lett. **76**, 3228 (1996).
[13] See Supplemental Material at http://link.aps.org/supplemental/10.1103/PhysRevLett.113.160504 for additional experimental details, and theoretical details regarding measurements on the compressed system, the "postselective disentanglement" simplification, a maximum likelihood analysis in the absence of data compression, and a simple calculation about the average measurement variance.
[14] M. Fiorentino and F. N. C. Wong, Phys. Rev. Lett. **93**, 070502 (2004).
[15] M. Fiorentino, T. Kim, and F. N. C. Wong, Phys. Rev. A **72**, 012318 (2005).
[16] J. T. Barreiro, T.-C. Wei, and P. G. Kwiat, Nat. Phys. **4**, 282 (2008).
[17] C. Vitelli, N. Spagnolo, L. Aparo, F. Sciarrino, E. Santamato, and L. Marrucci, Nat. Photonics **7**, 521 (2013).
[18] W.-B. Gao, C.-Y. Lu, X.-C. Yao, P. Xu, O. Gühne, A. Goebel, Y.-A. Chen, C.-Z. Peng, Z.-B. Chen, and J.-W. Pan, Nat. Phys. **6**, 331 (2010).
[19] L. A. Rozema, A. Darabi, D. H. Mahler, A. Hayat, Y. Soudagar, and A. M. Steinberg, Phys. Rev. Lett. **109**, 100404 (2012).
[20] S. Lloyd *et al.*, Phys. Rev. Lett. **106**, 040403 (2011).
[21] B. P. Lanyon, M. Barbieri, M. P. Almeida, T. Jennewein, T. C. Ralph, K. J. Resch, G. J. Pryde, J. L. O'Brien, A. Gilchrist, and A. G. White, Nat. Phys. **5**, 134 (2009).
[22] X.-Q. Zhou, T. C. Ralph, P. Kalasuwan, M. Zhang, A. Peruzzo, B. P. Lanyon, and J. L. O'Brien, Nat. Commun. **2**, 413 (2011).
[23] P. Seymour and T. Zaslavsky, Adv. Math. **52**, 213 (1984).
[24] R. B. A. Adamson, L. K. Shalm, M. W. Mitchell, and A. M. Steinberg, Phys. Rev. Lett. **98**, 043601 (2007).
[25] R. B. A. Adamson, P. S. Turner, M. W. Mitchell, and A. M. Steinberg, Phys. Rev. A **78**, 033832 (2008).
[26] G. Tóth, W. Wieczorek, D. Gross, R. Krischek, C. Schwemmer, and H. Weinfurter, Phys. Rev. Lett. **105**, 250403 (2010).
[27] D. M. Greenberger, M. A. Horne, and A. Zeilinger, *Bell's Theorem, Quantum Theory and Conceptions of the Universe*, edited by M. Kafatos (Kluwer Academic, Dordrecht, 1989), pp. 69–72.
[28] D. Bouwmeester, J.-W. Pan, M. Daniell, H. Weinfurter, and A. Zeilinger, Phys. Rev. Lett. **82**, 1345 (1999).
[29] W. Dür, G. Vidal, and J. I. Cirac, Phys. Rev. A **62**, 062314 (2000).